Reviewed research article

Location accuracy of earthquake hypocentres beneath Eyjafjallajökull, Iceland, prior to the 2010 eruptions

Jon Tarasewicz[1*], Robert S. White[1], Bryndís Brandsdóttir[2] and Bergthóra Thorbjarnardóttir[3]

[1]*Bullard Laboratories, University of Cambridge, Madingley Road, Cambridge, CB3 0EZ, UK*

[2]*Institute of Earth Sciences, Science Institute, University of Iceland, Askja, Sturlugata 7, 101 Reykjavík, Iceland*

[3]*Icelandic Meteorological Office, Bústaðavegur 9, 150 Reykjavík, Iceland*

**Corresponding author: jptt2@cam.ac.uk*

Abstract — *The depth of seismicity preceding the 2010 Fimmvörðuháls and Eyjafjallajökull eruptions in South Iceland has implications for the interpretation of the magma plumbing system that was active prior to those eruptions. Significant discrepancies exist in the hypocentral depths reported by different studies of the same earthquakes beneath Eyjafjallajökull in early-mid March 2010. Reported depths range from 3 km to 12 km. We use both real earthquake data and synthetic tests to show that the dominant factor controlling the best-fit hypocentral depths beneath the Eyjafjallajökull glacier is the network configuration. Hypocentral depths of 6–12 km are obtained when only data from permanent seismometer stations operated by the Icelandic Meteorological Office are used, the closest of which is located 13 km from the epicentral zone. Inclusion of data from six temporary seismometer stations deployed around Eyjafjallajökull, all within 4–15 km of the epicentral zone, constrains earthquake depths to be shallower than ∼6 km. A lack of proximal stations on top of the glacier limits resolution of earthquake sources that are shallower than ∼4 km, even when data from the six temporary stations are included. The choice of two plausible distinct velocity models has only a second-order effect on inferred hypocentral depths. We suggest that the true depth of seismicity is ∼2–6 km, which coincides with the depth of inflating magmatic intrusions inferred from surface deformation at that time.*

INTRODUCTION

In March–June 2010, Eyjafjallajökull volcano in South Iceland erupted first from a fissure on the eastern flank of the volcano at Fimmvörðuháls, then subsequently from a sub-glacial crater at the summit of the volcano (Figure 1). Both the Icelandic Meteorological Office's (IMO) published earthquake catalogue (e.g., Sigmundsson *et al.*, 2010, supplementary material) and Tarasewicz *et al.* (in press) report several thousand earthquakes with epicentres on the northeastern flank of the Eyjafjallajökull glacier during 5–20 March 2010. This activity immediately preceded the Fimmvörðuháls fissure eruption on 20 March.

However, whilst epicentral locations are in broad agreement, the reported hypocentral depths for these earthquakes show a consistent discrepancy between the two studies (Figure 2). Tarasewicz *et al.* (in press) find hypocentral depths predominantly at 3–6 km, whilst the IMO report depths predominantly in the range 7–11 km for the same seismic activity.

This study uses both real data and synthetic tests to explore the contribution to this depth discrepancy from variations in station distribution and in the assumed velocity structure. First, we test the effect in the hypocentral inversion of variation in network geometry resulting from the inclusion or exclusion of data from additional temporary seismometers. Sec-

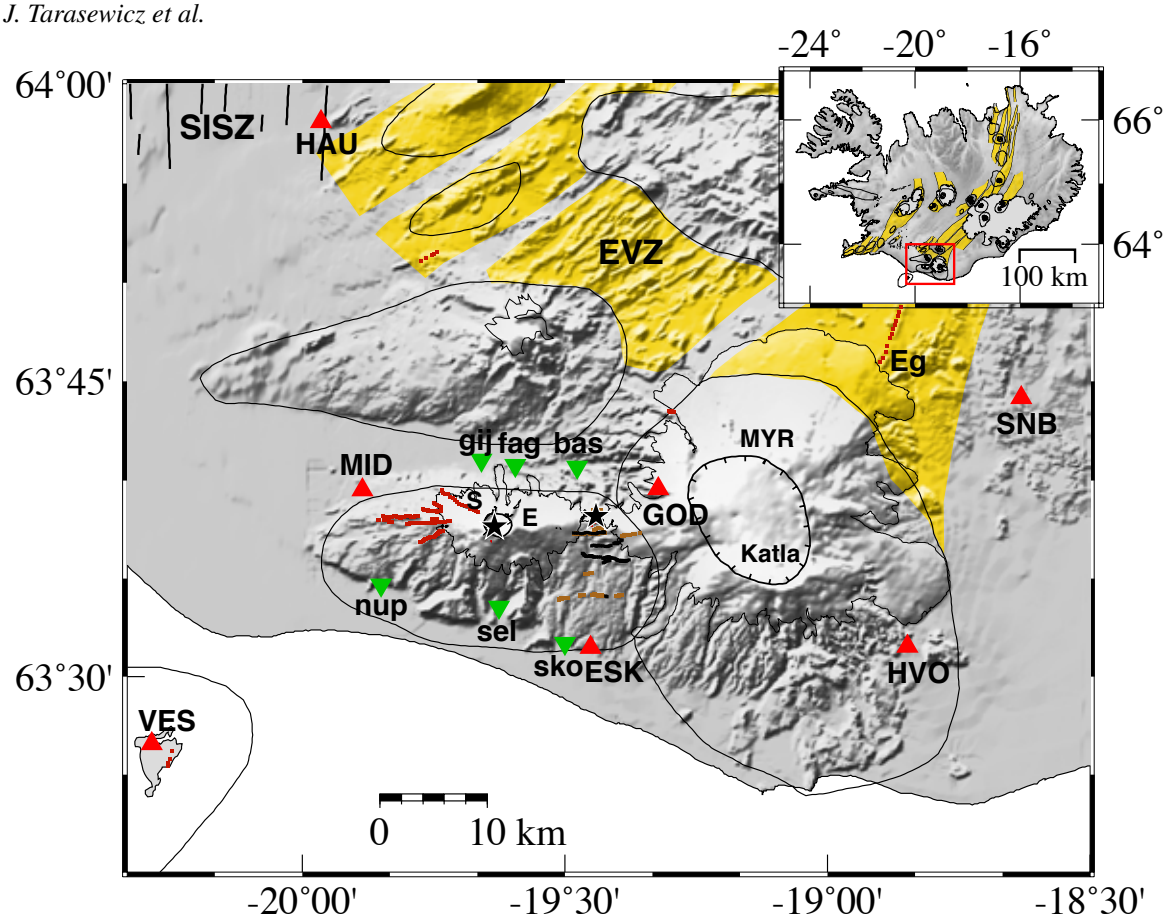

Figure 1. A tectonic map of the Eyjafjallajökull (E) and Katla volcanoes showing the seismic network configuration during early–mid March 2010. IMO-operated permanent seismometers are denoted by red triangles, with station names in capitals. Green inverted triangles are temporary seismometers. Black stars show the main craters of the March 2010 Fimmvörðuháls flank eruption and April–May 2010 Eyjafjallajökull summit eruption. Inset shows tectonic map of Iceland (Einarsson and Sæmundsson, 1987). Lighter grey-shaded areas show the extent of glaciers. Black lines indicate outlines of central volcanoes. Their associated fissure swarms are yellow-shaded. Tick-marked lines show outlines of summit craters and calderas. The Katla caldera lies beneath the Mýrdalsjökull (MYR) glacier. Faults are denoted by thick black lines, Holocene eruption fissures by red lines and older hyaloclastite ridges by brown lines. The NW striking Skerin ridge (S) formed in a composite 10th century eruption (Óskarsson, 2009). E-W aligned faults and fissures characterize Eyjafjallajökull (Jóhannesson and Sæmundsson, 2009; Einarsson and Hjartardóttir, in prep.). Eg – Eldgjá eruption fissure NE of the Katla caldera. Data from IMO station VAT (64.18664°N, 18.91768°W) were also used. – *Kort af eldstöðvakerfum Suðausturgosbeltisins (EVZ), teiknað eftir korti P. Einarssonar og K. Sæmundssonar (1987). Megineldstöðvar eru afmarkaðar með svörtum línum og sprungusveimar þeirra eru gulskyggðir. Goshryggir undan jökli eru brúnir en gossprungur á nútíma rauðar (skv. jarðfræðikortum H. Jóhannessonar og K. Sæmundssonar, 2009 og Birgis Óskarssonar, 2009). Jöklar eru gráskyggðir. Jarðskjálftamælistöðvar Veðurstofu Íslands eru merktar með rauðum þríhyrningum en færanlegar mælistöðvar umhverfis Eyjafjallajökul með grænum þríhyrningum. Svartar stjörnur sýna gosstöðvarnar á Fimmvörðuhálsi og í toppgíg Eyjafjallajökuls. Skerin (S) og Eldgjá (Eg).*

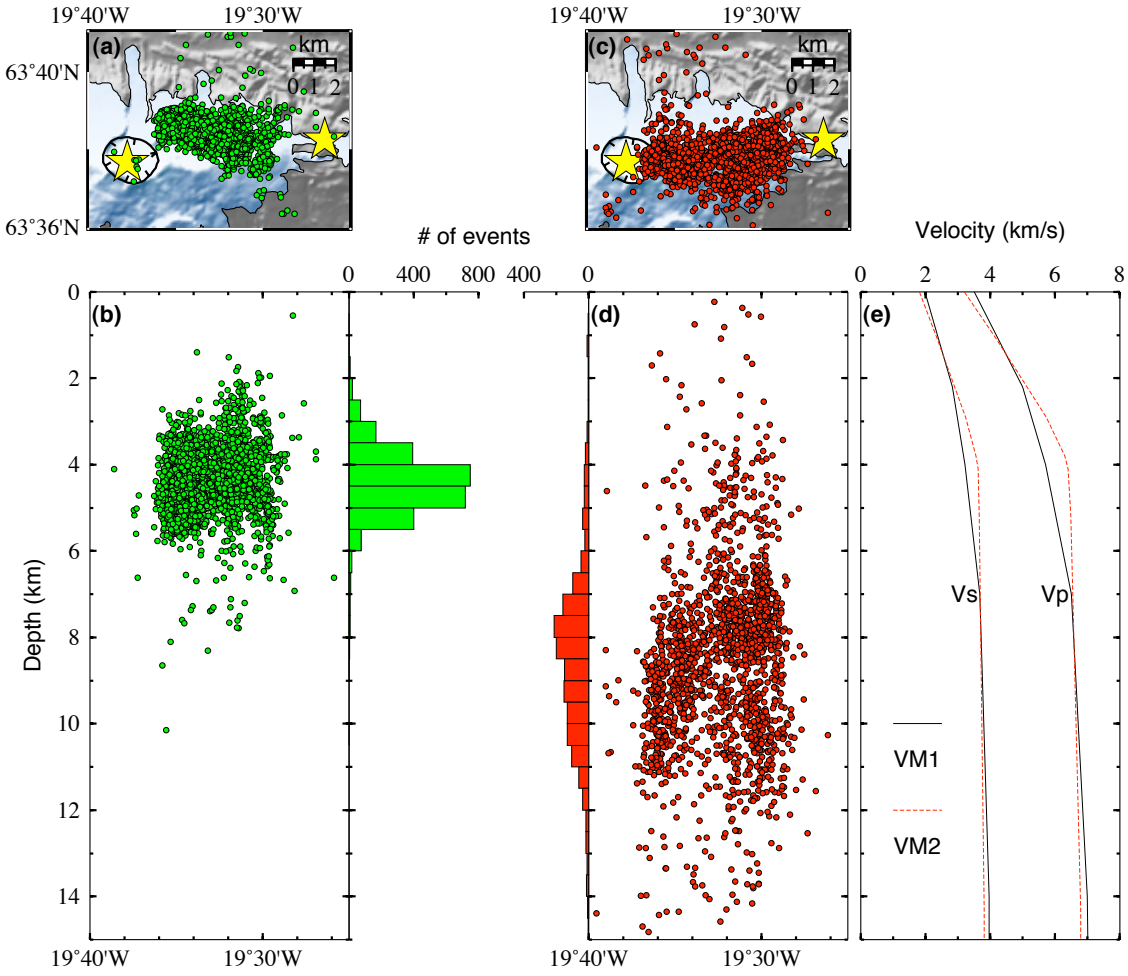

Figure 2. a) Epicentres of 2647 earthquakes detected using Coalescence Microseismic Mapping (CMM) during 6–20 March 2010 (Tarasewicz *et al.*, in press). (b) E-W cross-section (2x vertical exaggeration) showing the same events as in (a), and histogram showing that these lie predominantly in the 3–6 km depth range. Yellow stars in (a) and (b) show the flank (eastern star) and summit (western star) eruption sites, also shown in Figure 1. (c) 1749 epicentres from the IMO's earthquake catalogue for the same time period. Note that seismicity in (c) is shifted to the southwest compared to (a). (d) E-W cross-section (2x vertical exaggeration) and depth histogram showing IMO catalogue locations from (c), which lie predominantly in the 6–12 km depth range (e.g., Sigmundsson *et al.*, 2010). Depths in (b) are below sea level; depths in (d) are uncorrected depths reported in the IMO catalogue, which are relative to the nearest one or two seismic stations to an event (Martens *et al.*, 2010). (e) Velocity models compared in this study, *VM1* and *VM2*. V_p is P-wave (compressional) velocity, V_s is S-wave (shear) velocity. – *Upptakakort ásamt þversniði af 2647 jarðskjálftum 6.–20. mars, sem staðsettir voru með sjálfvirka CMM staðsetningarforritinu (grænfylltir hringir) og 1794 SIL-staðsettra skjálfta (rauðir hringir). Færanlegir mælar og SIL stöðvar voru notaðar við CMM staðsetningar. Dýptardreifing jarðskjálfta sem staðsettir eru með SIl stöðvum eingöngu er mun meiri (6–12 km) en þegar nærliggjandi stöðvum er bætt við (3–6 km). Tvö mismunandi hraðalíkön VM1 og VM2 (e) voru notuð til þess að kanna áhrif á upptakadreifingu skjálftanna. P-bylgjuhraði (V_p) og S-bylgjuhraði (V_s).*

ond, we consider the effect of using different velocity models to invert arrival time data.

Variation in network geometry

It is well established that, in order to place good constraints on earthquake hypocentres, a network ideally needs to have both good azimuthal coverage of the source and one or more stations close to the epicentre (e.g., Bondár *et al.*, 2004; Bai *et al.*, 2006; Martens *et al.*, 2010). Proximal stations are especially important for constraining the depth of earthquake sources. For ice-capped volcanoes such as Eyjafjallajökull, seismicity occurring directly beneath the glacier is rarely recorded by such an ideal network configuration, given the difficulties of seismic monitoring on glaciers.

Seismicity in Iceland is routinely monitored by the Icelandic Meteorological Office (IMO), which operates a permanent national network of seismometers. In early March 2010, the IMO network included three stations within 15 km of Eyjafjallajökull and another four within 50 km. Two weeks prior to the initial fissure eruption, the Institute of Earth Sciences, University of Iceland deployed an additional six seismometer stations around the base of Eyjafjallajökull (Figure 1). These temporary stations were all within 4–15 km of the epicentres of the main seismic activity during early–mid March 2010. Data from the more proximal temporary stations were combined with data from the IMO stations to obtain the hypocentre locations reported by Tarasewicz *et al.* (in press).

Variation in assumed velocity model

The velocity structure beneath Eyjafjallajökull has not been constrained directly by tomographic studies or refraction profiles that transect the edifice. Based on data from other similar volcanoes, Eyjafjallajökull is likely to have marked lateral variation in velocity structure, at least at shallow levels. There is therefore uncertainty regarding what velocity structure it is most appropriate to assume in calculating hypocentral locations. Tarasewicz *et al.* (in press) use a 1-D velocity model (*VM1*, see Figure 2e) based on the eastern end of the SIST refraction profile (Bjarnason *et al.*, 1993) and the northern part of the Katla refraction profile (Gudmundsson *et al.*, 1994). The SIST profile crossed the South Iceland Seismic Zone, with its easternmost shotpoint in the Gígjökull lake, at the central-northern margin of Eyjafjallajökull. The Katla profile lay NNW-SSE across Mýrdalsjökull, crossing the western Katla caldera. Both of these profiles report similar velocity gradients and increased upper crustal thickness in the vicinity of Eyjafjallajökull. A marked increase in upper crustal thickness is observed going east across the South-Iceland Seismic Zone into the Eastern Volcanic Zone (EVZ) (Bjarnason *et al.*, 1993; Pálmason, 1971). The depth below sea level to the 5.0 km/s isovelocity surface, which is a proxy for depth to the base of extrusive volcanics, is $\sim$2 km within the southern propagating tip of the EVZ. The depth to the 6.5 km/s isovelocity surface ranges from 5–10 km around Eyjafjallajökull (Brandsdóttir and Menke, 2008). The IMO use an alternative velocity model (*VM2*, Figure 2e) with slightly thinner uppermost crust and thus higher velocities in the 3–6 km depth range (Vogfjörð *et al.*, 2002). Both velocity models use a V_p/V_s ratio of 1.77 in the upper crust.

EARTHQUAKE DATA

We have used five earthquakes with local moment magnitudes (M_{lw}) greater than 2.5 (Table 1) as a sample to test the effects of varying the hypocentral location inversion parameters. All occurred under the northeastern flank of Eyjafjallajökull during March 2010 and all have hypocentres within the region of intense seismicity that occurred in the two weeks leading up to the Fimmvörðuháls eruption (Figure 2). The test events were some of the largest-magnitude earthquakes to occur around Eyjafjallajökull during March 2010 and all display clear P- and S-wave arrivals at all stations in the network that were operating at the time (Figure 3). This means that arrival time picks of the P-wave and S-waves are unambiguous. As such, these test events are both some of the best-constrained examples and are also representative of the several thousand other earthquakes that are found to be co-located within a consistent depth range, when a consistent set of location inversion parameters is employed.

We first use a Coalescence Microseismic Mapping (CMM) technique (Drew, 2010; Brandsdóttir *et al.*, 2010; Tarasewicz *et al.*, in press) to find hypocen-

Table 1. IMO earthquake locations used to test the effects of varying the hypocentral location inversion parameters. CMM depths are shown for comparison. – *IMO staðsetningar skjálfta sem notaðir voru til að meta skekkju staðsetningarforrita útfrá stöðvaneti og hraðalíkönum. Dýpi CMM staðsettra skjálfta er til samanburðar.*

date	time	latitude	longitude	IMO-depth	CMM-depth	M	M_{lw}
20100306	000838.212	63.63267	-19.59779	9.9	4.7	2.91	2.54
20100306	034246.008	63.63620	-19.59756	9.2	5.4	2.90	2.80
20100306	112047.226	63.63526	-19.60034	9.5	5.1	2.91	2.75
20100306	211711.247	63.64176	-19.58222	7.7	3.7	2.57	2.53
20100310	064312.106	63.63616	-19.60312	9.0	5.2	2.79	2.52

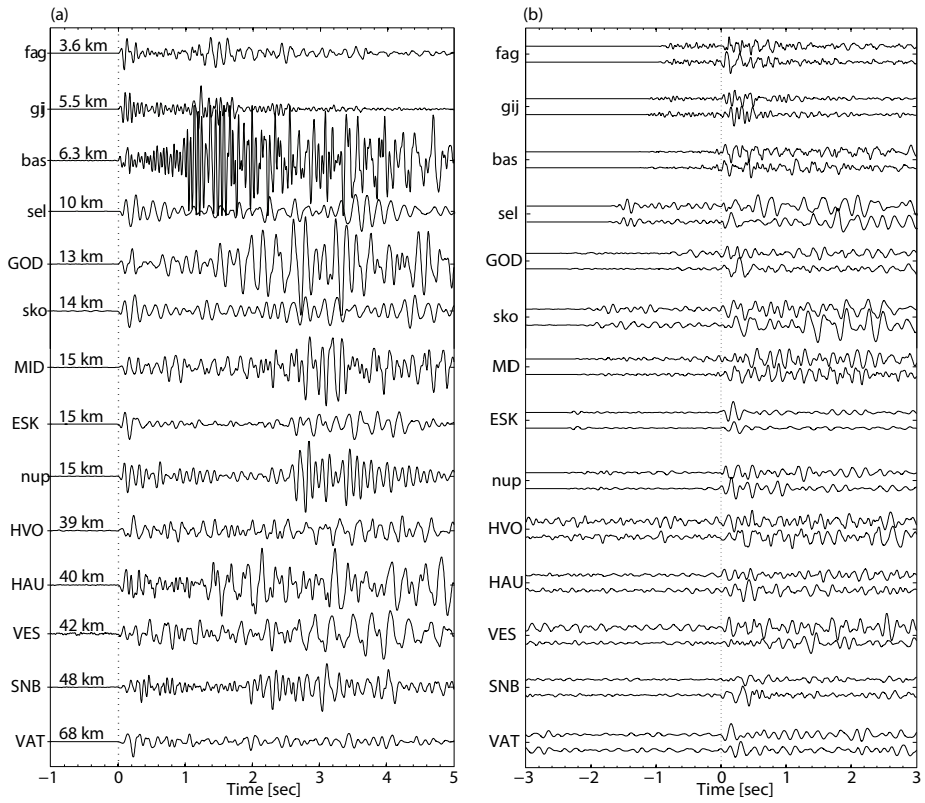

Figure 3. (a) Vertical-component waveforms from each seismometer station aligned by P-wave arrival for one of the five test events, which occurred at 06:43 on 10 March 2010, M_{lw}=2.5, ordered by epicentral distance (shown). (b) E–W (top) and N–S (bottom) horizontal-component waveforms for the same event, aligned on S-wave arrivals. Waveforms are trace-normalised on the P- or S-wave arrival respectively and bandpass filtered at 4–25 Hz. – *Flestir jarðskjálftanna undir Eyjafjallajökli í aðdraganda eldgossins á Fimmvörðuhálsi hafa skýrar P- og S-bylgjur, sbr. skjálftann 10. mars kl. 06:43, M_{lw}=2.5. Myndin til vinstri sýnir lóðrétta þátt hreyfingarinnar á hverri stöð og myndin til hægri láréttu þætti hreyfingarinnar (A-V og N-S). Lóðréttar línur sýna komutíma P- og S-bylgna.*

tre locations for the sample of real events using each combination of velocity model and network configuration (Figure 4). The CMM method was used to automatically detect and locate the hypocentres reported by Tarasewicz *et al.* (in press), using velocity model *VM1*.

The hypocentres at depths of 3–6 km obtained using CMM clearly illustrate the main conclusion of this paper: that the inclusion of data from the more proximal temporary stations places additional constraints on the hypocentral location, which require the earthquakes to be at relatively shallow depths. Using CMM, the variation in hypocentral depth caused by switching between the two different velocity models is a second-order effect by comparison, and cannot account for the discrepancy of ∼5 km between reported hypocentral depths. Hypocentral depths >6 km are only obtained when the temporary stations are excluded from the inversion. When this is the case, the closest remaining stations are ∼13–14 km away from the epicentres, and CMM returns hypocentral depths of 8–12 km (red circles in Figure 4).

To test this further, we manually picked P- and S-wave arrival times for our sample events and used Hypoinverse-2000 (Klein, 2002) to invert the arrival time picks using each combination of velocity model and network configuration. As with the CMM locations, we find that excluding the more proximal temporary stations from the inversion produces significantly deeper hypocentral depths of ∼10 km, for both velocity models (red circles in Figure 5). Again, we find that if the network geometry is unsuitable to constrain the depth of the earthquakes in the first place, then the choice of velocity model is secondary. However, when all stations are included in the inversion, velocity model *VM2* produces even shallower hypocentral depths of ∼2–4 km, and also increases the scatter of the hypocentres compared to the results using *VM1* (blue circles in Figure 5).

There is good agreement between hypocentral locations obtained using CMM and Hypoinverse when *VM1* is used in both cases (Figure 5a). However, when *VM2* is used, there is a discrepancy in hypocentral depth between CMM (∼4 km, Figure 4b) and Hypoinverse (∼2–4 km, Figure 5b) best-fit locations. We attribute this disagreement to the fact that Hypoinverse searches for a global minimum best-fit location, whereas CMM takes a weighted average of high-probability hypocentre locations for each event. The increase in scatter of locations with Hypoinverse and the disagreement between location methodologies hints that the earthquakes may be less well constrained when assuming velocity model *VM2* in the inversion.

SYNTHETIC TESTS

Methodology

To assess objectively the effects of network configuration at Eyjafjallajökull, we generated arrival times for synthetic earthquakes at varying depths with approximately the same epicentres as our real test events. The arrival times were derived using the travel-time look-up table generated during the CMM workflow for each velocity model. The look-up table contains P- and S-wave travel-times from each node in a search grid to every station in the network, calculated using a finite difference eikonal solver which takes account of the 3-D effects of varying station elevation. We compiled synthetic events with origins on a vertical string of nodes within the CMM search grid. The synthetic arrival time picks were then inverted using Hypoinverse, in the same way as the real data described above. In all the synthetic inversion tests presented in this paper, we used the exact arrival times from the forward modelling so as to highlight solely the effect of network configuration and choice of velocity model. The addition of characteristic random perturbations to the arrival times to simulate the effect of poor signal to noise ratios has the effect of increasing the scatter of the inverted hypocentral locations, but does not materially alter the effects of network or velocity model on a particular set of 'noisy' synthetic arrival time picks.

Synthetic arrival time picks were generated using both velocity models, *VM1* and *VM2* (Figure 2e). These were then inverted with different network configurations, using the same velocity model as was used to generate them, to test objectively the effect of network geometry. These synthetic arrival picks

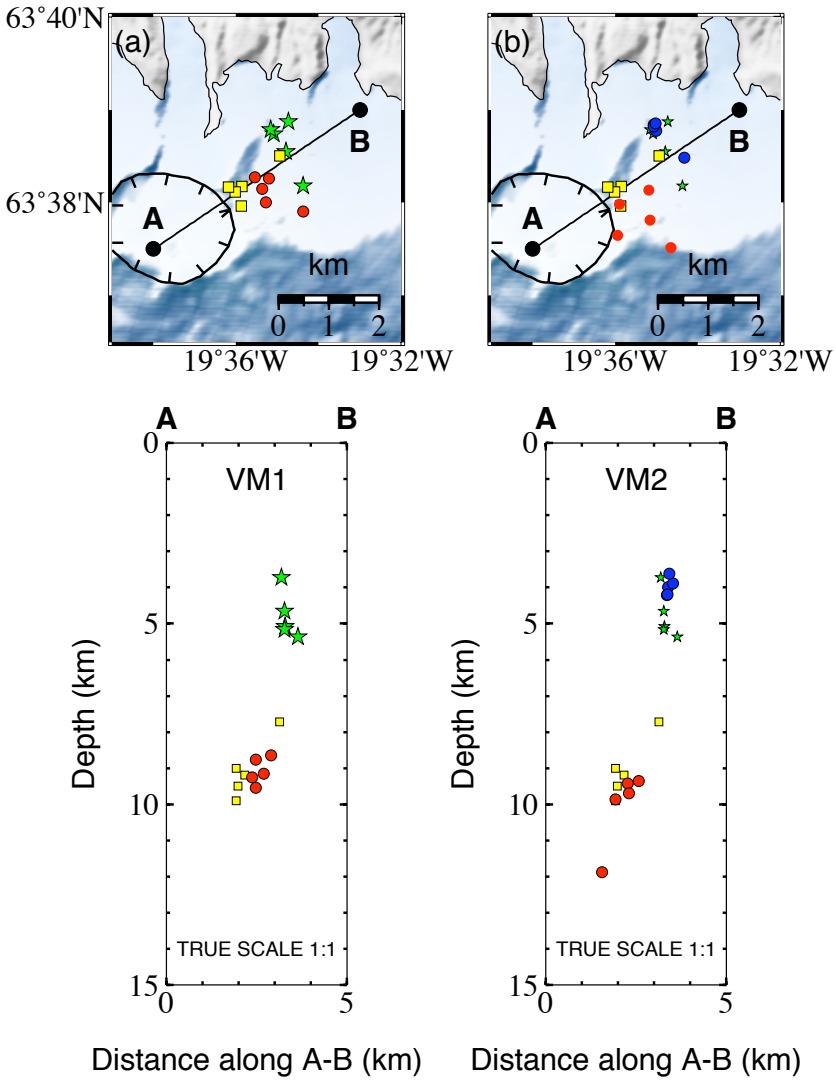

Figure 4. Maps and cross-sections showing hypocentre locations for the five test events obtained using CMM, assuming velocity model *VM1* (a) and *VM2* (b). Locations reported in the IMO catalogue (yellow squares) and by Tarasewicz *et al.* (in press) (green stars), are shown for reference in both (a) and (b). Blue circles are locations obtained using all stations (not shown in (a), since they are identical to the green stars, which were obtained using *VM1* and all stations). Red circles are locations obtained when data from the temporary stations are excluded. – *Upptakakort fimm jarðskjálfta sem staðsettir voru með mismunandi stöðvanetum og hraðalíkönunum VM1 og VM2. Gulir ferningar sýna staðsetningar SIL-kerfisins og rauðir hringir CMM staðsetningar með SIL stöðvum. Þegar færanlegu mælunum er bætt við verða staðsetningarnar áberandi grynnri. CMM staðsetningar með VM1 hraðalíkaninu (grænar stjörnur) eru aðeins dreifðari en VM2 staðsetningar (bláir hringir).*

were also inverted using the 'wrong' velocity model (i.e., not the one used to calculate the synthetic arrival times), to provide some insight into the effect of using a velocity model for inversion that does not match the true velocity structure, which is inevitably the case to some extent in real situations.

As well as the two network configurations that are simply 'including' or 'excluding' all the temporary stations, we also ran inversions excluding the IMO station VES, which is located offshore, on the Vestmannaeyjar islands (Figure 1). This is relevant because the time residuals reported by Hypoinverse for arrivals at VES for the real test events are frequently so large (i.e., the arrivals are late compared to the modelled time) that they are significantly downweighted or excluded from the final iterations of the location inversion. In addition, our experience is that it is only possible to pick arrivals confidently at VES for the largest Eyjafjallajökull events. For the majority of earthquakes plotted in Figure 2 we would not expect to obtain high-quality arrival time picks from VES. It is therefore important to test what effect it has when the station is excluded completely from the synthetic tests. In fact, when VES is excluded, the effect is to 'push' synthetic hypocentral locations even deeper and to the southwest, away from the true source depth (Figure 6).

Synthetic test results

A synthetic hypocentre at 5 km depth is reliably recovered using all stations and the same velocity model as was used to create it (blue circles in Figure 6). However, consistent with our real test events, when the synthetic arrival times are inverted using a sparser network that excludes the temporary stations, the best-fit hypocentre is significantly deeper than the true synthetic source (red open circles in Figures 6b and 6e). It also has larger location uncertainties reported by Hypoinverse. The same is also true for a synthetic source event generated at 10 km depth (Figures 7b and 7e).

The shift in epicentral location that results from using a sparser network is less marked than the effect on depth. Nonetheless, there is a clear shift to the southwest when the proximal temporary stations are excluded. This effect is even greater when the IMO seismometer station VES is also excluded, which leaves a large azimuthal gap of $\sim$125° to the southwest (pink symbols, Figures 6 and 7).

When the synthetic arrival times for sources at 5 km and 10 km depth are inverted using the 'wrong' velocity model (that is, whichever of *VM1* or *VM2* was not used to generate them), this has relatively little incremental effect on the poorly constrained, artificially deep hypocentres that are obtained when data from the proximal temporary stations are excluded. Approximately the correct source location is retrieved for the 10 km deep source if all the stations are used, even when the 'wrong' velocity model is used in the inversion. This suggests that the choice of *VM1* or *VM2* has only a limited effect on the best-fit hypocentral location for sources at that depth (Figure 7).

More significantly, there is a substantial discrepancy between the synthetic source and best-fit hypocentre when the 'wrong' velocity model is used to invert for the 5 km deep source. This is not surprising, given that most of the variation in the velocity models occurs in the top 6 km. The effect of using *VM2* to invert synthetic arrivals calculated for a source at 5 km depth within *VM1* is to obtain an apparent hypocentral depth of 1.8 km (Figure 6c). The sense and scale of this mismatch is similar to that observed when the real data from our test events is inverted using *VM2* as compared with *VM1* (Figure 5b). The reverse situation (using *VM1* to invert synthetic arrivals generated for a source at 5 km depth within *VM2*) produces a best-fit location of 6.3 km (Figure 6f), which does not match the behaviour of the inversions of the real test events.

Network resolution at shallow depths

To understand better the behaviour at shallow depths of both the real and synthetic data, a series of synthetic sources was created from the surface down to 15 km and inverted as described above, again assuming that exact P- and S-wave travel times are known (Figure 8).

Even when the true velocity model is used to invert the synthetic arrival times using all available stations, Hypoinverse does not resolve the true source depth if it is shallower than $\sim$4 km for *VM1* and

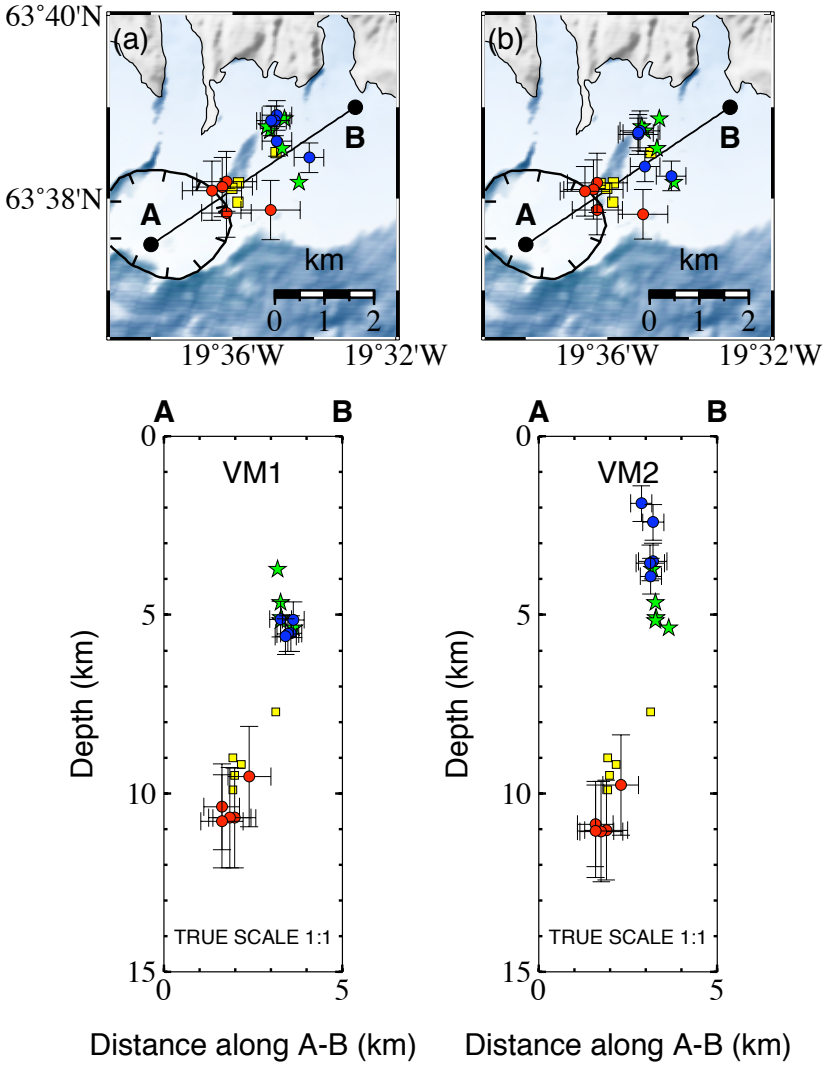

Figure 5. Maps and cross-sections showing hypocentre locations for the five real test events obtained using Hypoinverse. Labels as in Figure 4. Error bars are reported errors in Hypoinverse. Hypoinverse depths are relative to the mean station elevation (240 m for all stations, 320 m for the network excluding temporary stations). – *Hypoinverse staðsetningar sömu jarðskjálfta og á 4. mynd, með reiknaðri óvissu. Með færanlegu mælunum verða CMM sem og Hypoinverse staðsetningarnar grynnri hvort sem VM1 eða VM2 hraðalíkanið er notað.*

~3 km for *VM2* (Figure 8a–b). We attribute this behaviour to the fact that, at very shallow depths, the network is poorly configured to provide good depth constraint even in the case where the more proximal temporary stations are included. This point can be demonstrated by including an additional virtual station directly above the synthetic sources in the inversion. The 'enhanced' network including the extra virtual station successfully recovers the true depths of the synthetic sources to the very shallowest levels.

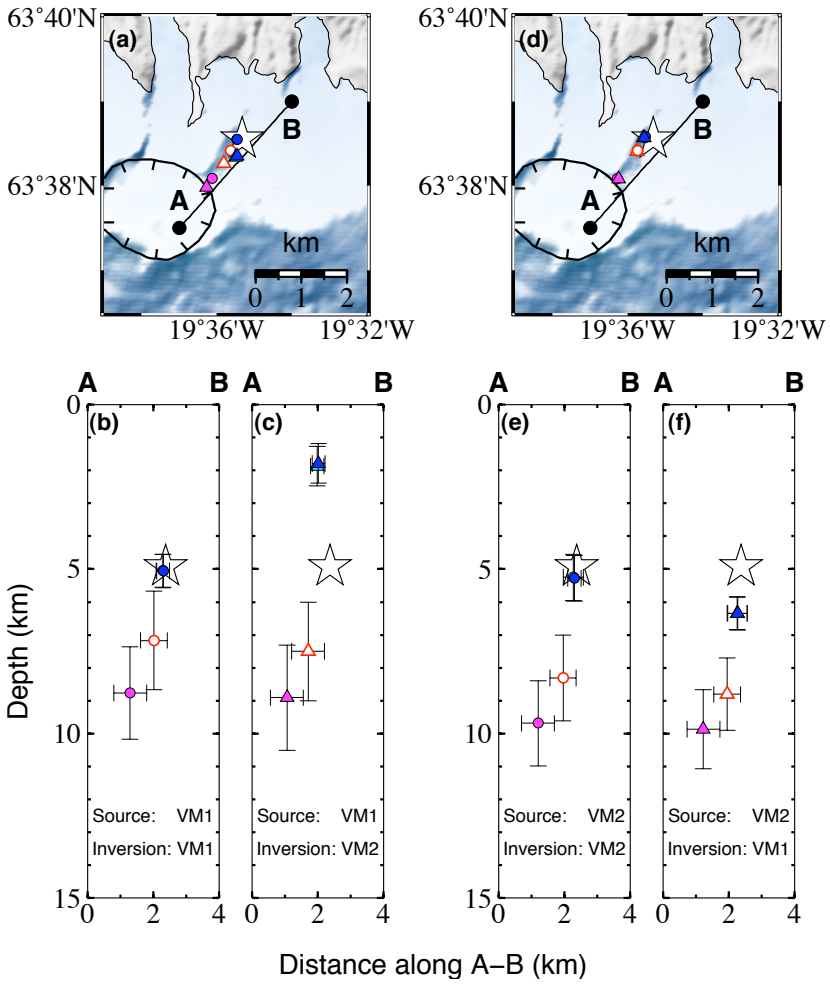

Figure 6. Maps and cross-sections showing the results of hypocentral inversion of arrival times calculated for a synthetic event at 5 km depth (black star). (a–c) show results of inverting synthetic arrival times that were calculated using *VM1*, then inverted using *VM1* (circles in (a) and (b)) and *VM2* (triangles in (a) and (c)). (d–f) show the same tests, but for synthetic arrival times calculated using *VM2*, then inverted using *VM2* (circles in (d) and (e)) and *VM1* (triangles in (d) and (f)). Dark blue – hypocentres using all stations. Light blue – hypocentres using all stations except VES (mostly hidden under dark blue). Red open circles/triangles – hypocentres excluding all temporary stations. Pink – hypocentres excluding both the temporary stations and VES. Cross-sections have vertical scale 1:1. – *Staðsetningar tilbúins skjálfta á 5 km dýpi (hvít stjarna) með reiknuðum upptakatíma úr hraðalíkönunum VM1 og VM2. Staðsetning með öllum stöðvunum (dökkbláir hringir/þríhyrningar), öllum stöðvum utan Vestmanneyjum (VES), (ljósbláir hringir/þríhyrningar), SIL stöðvum eingöngu (rauðir hringir/þríhyrningar) og SIL stöðvum án VES (lillabláir hringir/þríhyrningar). Með VES verða SIL staðsetningarnar grynnri. VES hefur hins vegar lítil sem engin áhrif á staðsetningarnar þegar færanlegu stöðvarnar eru hafðar með.*

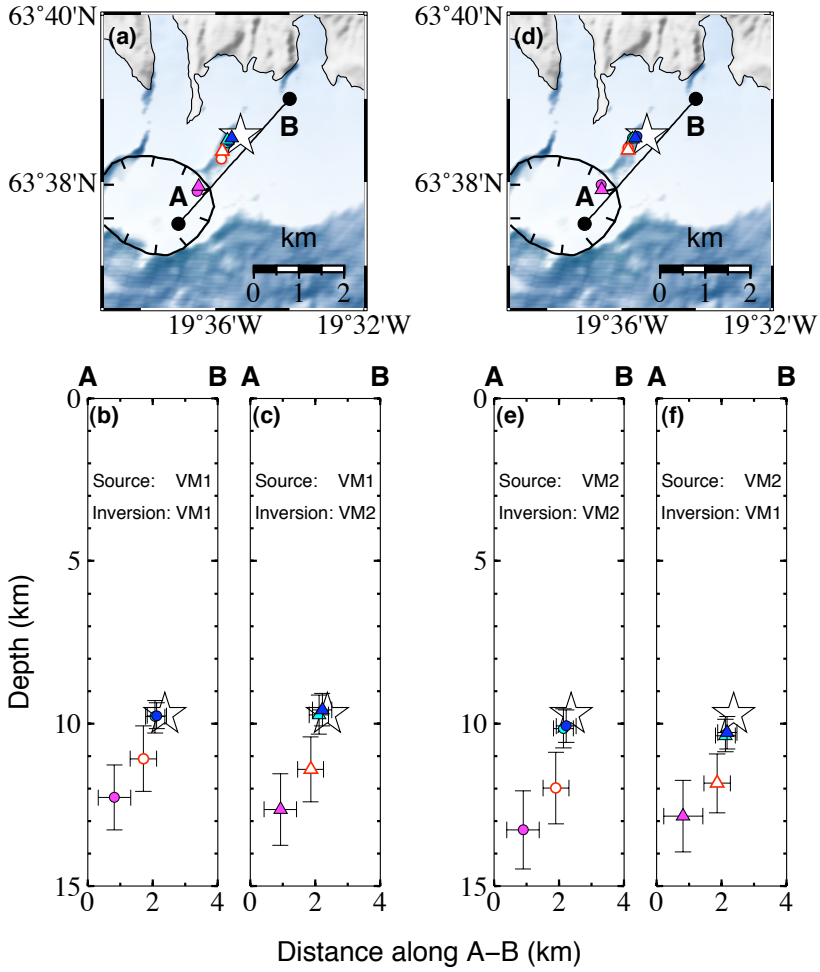

Figure 7. Maps and cross-sections showing the results of hypocentral inversion of arrival times calculated for a synthetic event at 10 km depth (black star). (a–c) show results from inverting synthetic arrival times that were calculated using *VM1*, then inverted using *VM1* (circles in (a) and (b)) and *VM2* (triangles in (a) and (c)). (d–f) show the same tests, but for synthetic arrival times calculated using *VM2*, then inverted using *VM2* (circles in (d) and (e)) and *VM1* (triangles in (d) and (f)). Colour code as in Figure 6. Cross-sections have vertical scale 1:1. – *Staðsetningar tilbúins skjálfta á 10 km dýpi (hvít stjarna) með reiknuðum upptakatíma úr VM1 og VM2. Litaskali eins og á 6. mynd.*

The results also illustrate the consistent overestimation of source depth when the temporary stations are excluded from the inversion (open red circles in Figure 8). This effect is exacerbated when the permanent station VES is also excluded (pink circles in Figure 8), as is often the case for the real data.

At no synthetic source depth does Hypoinverse find best-fit locations shallower than 3–4 km, if the 'correct' velocity model is used to invert the synthetic arrivals. Shallower depths appear to be precluded as solutions by the network geometry when 'perfect' synthetic arrivals are used. However, when

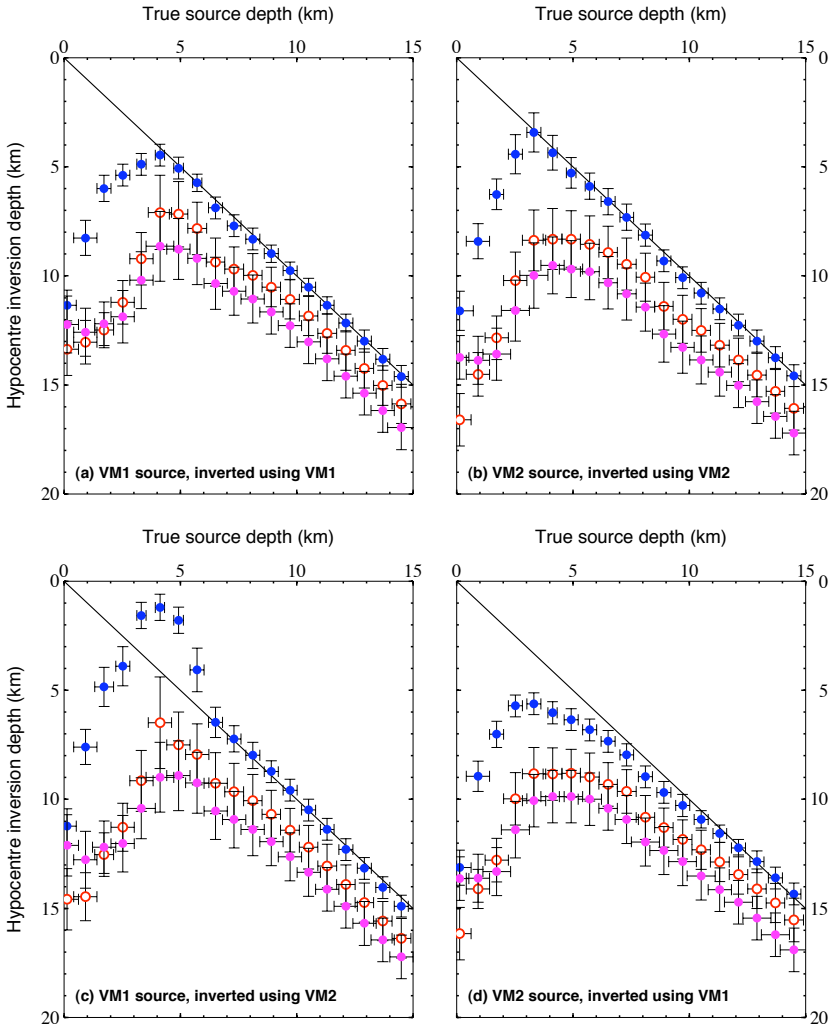

Figure 8. Plots of hypocentral best-fit locations obtained when inverting arrival times for synthetic events with true depths between 0–15 km. Color code as in Figure 6. Error bars are reported errors from Hypoinverse. (a) and (b) show synthetic arrivals inverted using the same velocity model as was used to generate them (*VM1* and *VM2* respectively). (c) and (d) show the effect of using the 'wrong' velocity model to invert synthetic arrival times (see text for discussion). – *Samanburður á Hypoinverse staðsetningum tilbúinna jarðskjálfta á 0–15 km dýpi. Litaskali Hypoinverse staðsetninga samkvæmt 6. mynd. Hypoinverse ræður ekki við staðsetningar skjálfta grynnri en 3–4 km með öllum stöðvum (bláir hringir) og grynnri en 7 km með SIL stöðvunum eingöngu. Frávik mælaneta minnka með dýpi. Reiknuð óvissa í staðsetningum minnkar með auknum fjölda mælistöðva. Þegar reiknuðum ferðatímum er víxlað á milli hraðalíkana (neðri myndir) verða dýptarákvarðanir Hypoinverse óreglulegri í efstu 5 km.*

the 'wrong' velocity model *VM2* is used to invert the synthetic arrival times generated using *VM1*, Hypoinverse does find best-fit locations which are shallower than the synthetic sources, if the true source depth is between 3–6 km depth (Figure 8c). This is the depth range with the greatest contrast between the two velocity models, with *VM2* having higher velocities than *VM1* for these depths (Figure 2e). Conversely, when *VM1* is used to invert synthetic arrivals generated using *VM2*, the resultant hypocentre depths are consistently 'too deep' for synthetic sources shallower than ∼10 km (Figure 8d). Synthetic source depths of ∼7 km or deeper are recovered to within ±1 km when inverted using either velocity model, suggesting that deeper real sources should be well constrained and relatively insensitive to the assumed velocity model.

DISCUSSION

Effects of changing network geometry

Our synthetic tests and inversion of real data all show that when data from the temporary stations is excluded from the location inversion, best-fit hypocentral depths are deeper than those obtained when all stations are used in the inversion. This is a clear illustration of the importance of proximal stations in constraining the depth of earthquakes. The temporary stations also improve the azimuthal coverage of the network for seismicity in the active region under the northeast flank of the glacier.

The exclusion of the permanent station VES has a further, consistent 'deepening' effect on hypocentral solutions for true sources deeper than ∼3 km and is likely to reflect better the reality for most events in the active region. This effect on depth is minor (<0.5 km) if the temporary stations are included in the network, but acts to increase the best-fit hypocentral depth by 1–2 km if only the permanent IMO stations are used.

At shallow depths beneath the glacier, where there are no stations directly overhead to provide good depth constraint, network geometry becomes a limiting factor even if all available stations are included in the hypocentral inversion. Figure 8 illustrates that there is a characteristic depth, determined by the velocity model (4 km for *VM1*, 3 km for *VM2*), shallower than which source depths cannot be well resolved by the Eyjafjallajökull network for earthquakes occurring under the northeast flank of the glacier.

Besides having a dominant effect on the depth of hypocentral locations, the more proximal temporary stations also provide better azimuthal coverage. The configuration of the network when the temporary stations are excluded leaves an azimuthal gap to the southwest of ∼125° between the relatively proximal stations MID and ESK, which is filled only by the more distant station VES (Figure 1). The result of excluding data from the temporary seismometers is to shift epicentres to the southwest from the true synthetic location in every case we have shown (Figures 6 and 7). Even with 'perfect' synthetic arrival times, the relative weakness in coverage on the southwest side of the network appears to preclude good constraint along a northeast-southwest axis. The hypocentres of the real test events obtained using only the sparser permanent network are also located to the southwest of those obtained when data from all seismometers are included (Figure 5). This southwestward shift can also be seen clearly for the wider catalogue of seismicity in this locality during this period (Figure 2c vs. 2a).

When data from station VES are also excluded, the constraints on the position along this northeast-southwest axis become markedly poorer. When this is the case, the inversion tends to converge on apparent epicentral locations even further to the southwest, ∼1.5 km away from the true source's epicentre for the synthetic sources shown at 5 km and 10 km depth in Figures 6 and 7.

At what depth are the real earthquakes?

Our results show that hypocentral depths of 7–11 km for our test events are artificially deep and are a consequence of sub-optimal network geometry, only obtained when data from the temporary stations are excluded (Figures 4–6 and 8). The only scenario in which true depths of 7–11 km could be consistent with the real and synthetic results is if the true 3-D velocity structure is sufficiently different to both *VM1* and *VM2* in such a way that the velocity structure along ray-paths to the proximal temporary stations means that their inclusion in the inversion skews results to ar-

tificially shallow levels. This would imply unusually high velocities above the source region, distributed such that travel times were reduced significantly to the proximal temporary stations but not to the more distant permanent stations. We view this interpretation as unnecessarily convoluted and unlikely compared to the simpler interpretation that the deep locations inferred by using only the more distant stations are the result of sub-optimal network geometry.

Our analysis also disproves the notion that the true depth of seismicity is ∼10 km, and that artificially shallow hypocentres at ∼5 km might simply be the result of switching between *VM1* and *VM2*. Rather, the choice of velocity model is shown to be only a secondary factor in determining the hypocentral depth in this situation.

Instead, our synthetic tests and inversions of the earthquake data when the temporary stations are included indicate that the true depth of our test events is shallower than 6 km. Inverting arrival times from our real sample earthquakes using our preferred parameters (velocity model *VM1* and including data from all available stations) returns hypocentral depths of 5–6 km (Figure 5a). However, Figure 8a shows that even if *VM1* is a good approximation of the true velocity structure, hypocentral depths of 5±1 km would be found for all true source depths in the range ∼2–6 km. This is because the geometry of the network limits its resolution at shallow depths, even when data from all stations are included in the inversion.

On the other hand, inverting the arrival times from our real sample earthquakes using *VM2* returns hypocentral depths of 2–4 km (Figure 5b). However, we have shown that hypocentral depths shallower than ∼4 km are not well constrained by the network in this epicentral region, even when data from all stations are included. The only scenario in which our synthetic tests produce best-fit hypocentres at such shallow depths is when a velocity model that deviates from the true velocity structure is used to invert the data. In that scenario, the best-fit hypocentral locations are in fact too shallow compared to the true source depths. For the specific case in which synthetics generated using a true velocity model *VM1* are inverted using the 'wrong' *VM2*, the shallow hypocentres found for the real data (using *VM2*, Figure 5b) match the artificially shallow depths of synthetic hypocentres for true source depths of ∼2–6 km (Figure 8c). Therefore, the behaviour of the hypocentral solutions for the real test data when inverted with both *VM1* and *VM2* is consistent with the true earthquake hypocentres lying within the 2–6 km depth range. Whilst not conclusive, the synthetic tests suggest that the more scattered hypocentral solutions in the ∼2–4 km depth range for the real test events are likely to be poorly constrained and may hint at material deviations from the true velocity structure in velocity model *VM2*.

Therefore, whilst the synthetic and real data clearly indicate that the true depths of our test events are <6 km, it is harder to distinguish between well resolved hypocentres of true sources at ∼4–6 km depth and apparent hypocentral locations in the same 4–6 km depth range that derive from earthquakes with true source depths of 2–4 km. The observed pattern of hypocentral depths obtained by inverting the earthquake data with *VM1* (5–6 km) and *VM2* (2–4 km) could be obtained either for well resolved true sources at 5–6 km depth, or for incorrectly located true sources at 2–3 km depth (Figures 8a and 8c). Our synthetic tests suggest that true sources shallower than ∼2 km would have apparent hypocentral locations at depths >6 km and therefore should be distinguishable from true sources in the 2–6 km depth range.

On the basis of seismic data alone, we cannot conclusively say whether our test events really are well resolved at ∼5 km depth, as suggested by inversion using our preferred parameters (Figure 5a). However, this remains our preferred interpretation (compared to the alternative interpretation that the true sources are at 2–3 km depth) because it is in agreement with the position of a sill inferred from surface deformation data to be inflating at 4–6 km depth (Sigmundsson *et al.*, 2010). These authors also model an inflating dyke (in combination with the sill) to fit the surface deformation observations. This modelled dyke extends to very shallow levels (10s to 100s of metres from the surface), and hence may be consistent with the observed seismicity being towards the shallower end of the 2–6 km depth range. However, the modelled dyke is located towards the eastern end of the seismically

active zone, and does not coincide spatially with our test events.

We conclude that the most likely depth range for our test events is in fact at 5–6 km depth, and that they are well resolved at this depth, but we note that there is a risk that they may be shallower than this, within the ∼2–6 km depth range. A 2–6 km depth range is consistent with both our synthetic tests and real earthquake data. If the true source depths were deeper than this, they should be well resolved by including data from all available stations, and depths should not vary by more than ∼1 km between velocity models. If the true source depths were shallower than ∼2 km, the synthetic tests suggest that Hypoinverse best-fit locations would 'flip' to artificially deep hypocentres (>6 km) due to non-ideal network geometry.

We caution that we have only run tests for *VM1* and *VM2*, each being a plausible velocity model for the Eyjafjallajökull region that has been implemented in previous studies. We have not tested the range of other plausible 1-D approximations to the true velocity structure. Also, some degree of 3-D variation in the true velocity structure is highly probable, particularly at shallow depths. Hence we cannot rule out the possibility that the true hypocentral depths are in fact shallower than our preferred ∼2–6 km range. This might be the case if deviations from the true shallow velocity structure cause Hypoinverse to converge on best-fit depths that match our observations for the real data (∼5 km or ∼2–4 km for *VM1* and *VM2* respectively), when the true depth is <2 km. This would contrast with the prediction of our synthetic tests that such shallow true event depths would produce much deeper best-fit hypocentres (>6 km) in Hypoinverse if either of *VM1* or *VM2* is a good approximation to the true velocity structure.

Implications for interpretation of the seismic activity before the eruptions

Our five test events are some of the best-constrained examples from several thousand earthquakes recorded during early–mid March 2010 that broadly co-locate in depth, if consistent inversion parameters are used. Epicentres for these earthquakes predominantly lie within 5 km of our test events. Source-network geometry does not change materially over the epicentral zone on the northeast flank of the glacier where these events are located (Figures 1 and 2).

We infer that the majority of the several thousand events detected during 5–20 March 2010 also occurred at ∼2–6 km depth, based on our conclusions for the depth of the real test events used in this study.

The seismicity is likely to be the result of high strain rates caused by magma movement through the crust prior to the Fimmvörðuháls and Eyjafjallajökull eruptions (Tarasewicz *et al.*, in press). Estimates of magma migration paths, ascent rates and intrusion locations are dependent on determining accurately the location, particularly depth, of seismicity.

Magma flux into an intrusion complex at ∼2–6 km depth under the northeast flank of Eyjafjallajökull, in the region of hypocentres found using data from all available stations (Figures 2a and 2b), is consistent with the depth and location of deformation sources inferred by modelling surface deformation during this period (Sigmundsson *et al.*, 2010). The epicentral locations found when using only data from IMO seismometers (Figure 2c) also lie predominantly within the outline of the modelled deformation source. However, these epicentres are biased towards the southern edge of the modelled inflation source and some extend beyond its western boundary, compared to epicentres found using all stations, which lie closer to the centre of the modelled inflation source (see Figure 3 of Sigmundsson *et al.*, 2010). This is consistent with epicentral locations in Figure 2c being south to southwest of their true sources.

CONCLUSIONS

(1) The dominant factor in determining hypocentral depths at Eyjafjallajökull is network geometry. Our synthetic tests and real data show that excluding the more proximal temporary stations from the location inversion always results in best-fit hypocentral locations that are artificially deep. We conclude that this is the main factor behind the discrepancy between hypocentral depths reported from different studies.

(2) The network geometry around Eyjafjallajökull cannot resolve earthquake depths shallower than ∼4 km, even when all available stations are included in

the inversion. This is because there are no seismic stations directly above the seismicity, which would be necessary to constrain depths right up to near-surface levels.

(3) The real data and synthetic tests are consistent with the true earthquake depths being in the range ∼2–6 km below sea level under the northeast flank of the Eyjafjallajökull glacier. Our preferred locations for the five real test events are all at 5–6 km depth. However, synthetic tests indicate that events with true depths of ∼2–5 km depth could also result in hypocentral best-fit solutions at ∼5–6 km depth using Hypoinverse. Hence we cannot resolve with confidence where the real sources are within the 2–6 km depth band. If the true source depths were deeper than this, they should be well resolved by including data from all available stations, and depths should not vary by more than ∼1 km between velocity models. Conversely, if the true source depths were shallower than ∼2 km, synthetic tests suggest that Hypoinverse best-fit locations would 'flip' to artificially deep hypocentres due to non-ideal network geometry.

(4) Several thousand other earthquakes detected during the two weeks preceding the Fimmvörðuháls eruption in March 2010 are likely to have been predominantly in the same ∼2–6 km depth range. These events broadly co-locate in depth with the five test events used in this study, if consistent inversion parameters are used. Most epicentres are within 5 km of our test events under the northeast flank of the Eyjafjallajökull glacier, and source-receiver geometry does not change materially over that distance within the epicentral zone. We interpret this seismicity as being associated with the inflation of an intrusion complex at similar depth to the seismicity, in agreement with the inferred depth of inflation sources derived from surface deformation modelling.

(5) Variation in the assumed velocity model has a secondary effect on locations. We have shown how important the temporary proximal stations are for constraining the depth of earthquake hypocentres. If all stations are included in the inversion, our synthetic tests show that, for earthquake sources deeper than ∼7 km, inversion using either velocity model (*VM1* or *VM2*) returns approximately the true source depth (to within ±1 km). This is true, independent of which velocity model is used to create the synthetic arrival times. Only at depths shallower than ∼5 km do the velocity models *VM1* and *VM2* produce significant variation in best-fit hypocentral depths, if the 'wrong' velocity model is used to invert synthetic events. At these depths, the sub-optimal network geometry is already beginning to limit the ability to constrain earthquake depth in any case.

Acknowledgements

The temporary stations used in this study are from the LOKI instrument pool, which is jointly owned by the Icelandic Meteorological Office, the Institute of Earth Sciences, Univ. of Iceland and the Iceland GeoSurvey. We thank Martin Hensch, Sveinbjörn Steinþórsson, Þorsteinn Jónsson, Ólafur Guðmundsson, Benedikt Ófeigsson and numerous other scientists and graduate students who helped with the Eyjafjallajökull fieldwork. We also thank the landowners at Seljavellir and Núpar for housing the seismic stations sel and nup. The Icelandic Coast Guard helicopter was used to retrieve the gij station following the floods from Gígjökull on April 14th 2010. Julian Drew wrote the CMM software and Hilary Martens developed the Matlab code used for arrival time picking. Finnur Pálsson, Eyjólfur Magnússon and Ásta Rut Hjartardóttir provided digitized data of glacier outlines, eruption sites and tectonic features. Generic Mapping Tools (Wessel and Smith, 1998) were used to produce the figures. We acknowledge thoughtful reviews by Egill Hauksson and Heidi Soosalu. J. T. is funded by a NERC studentship and CASE award supported by ERC Equipoise Ltd. Dept. Earth Sciences, Cambridge, contribution number ESC2249.

ÁGRIP

Mat á nákvæmni í staðsetningum jarðskjálfta undir Eyjafjallajökli, í undanfara gossins á Fimmvörðuhálsi í mars 2010.

Nákvæmni í staðsetningum jarðskjálfta er háð þéttleika stöðvanetsins og breytileika í bylgjuhraða jarðskorpunnar. Mikilvægt er að ákvarða upptakadýpi jarðskjálfta innan eldfjalla til þess að fá hugmynd

um hversu nálægt yfirborði kvikan er. Í þeim tilgangi voru settir út 6 færanlegir jarðskjálftamælar umhverfis Eyjafjallajökul 6. og 8. mars 2010 (1. mynd). Þegar fyrstu gögnum var tappað af mælunum, viku seinna, varð ljóst að upptök jarðskjálftanna voru mun grynnri en sjálfvirkar mælingar SIL-kerfisins gáfu til kynna, á 3–6 km dýpi í stað þess að vera á yfir 7 km dýpi. Sjálfvirkar staðsetningar 2647 jarðskjálfta, 6.–20. mars undirstrika þennan mun (2. mynd). Skjálftar staðsettir með færanlegum mælaneti og SIL stöðvum eru bæði grynnri og liggja norðar en skjálftar sem staðsettir eru með SIL stöðvum eingöngu. Flestir jarðskjálftanna undir Eyjafjallajökli í aðdraganda eldgossins á Fimmvörðuhálsi hafa skýrar P- og S-bylgjur (3. mynd). CMM- og Hypoinverse staðsetningar á fimm stærstu skjálftunum með SIL-stöðvum eingöngu ber vel saman við SIL-staðsetningarnar, skjálftarnir lenda einnig neðan 7 km dýpis. Með færanlegu stöðvunum til viðbótar verða staðsetningarnar hins vegar mun grynnri, óháð því hraðalíkani sem notað er (4. og 5. mynd). *VM1* hraðalíkanið er byggt á bylgjubrotsmælingum vestan og austan Eyjafjallajökuls, sem sýna að efri hluti skorpunnar er mun þykkari og bylgjuhraði því lægri undir suðausturgosbeltinu miðað við Suðurlandsundirlendið. SIL-kerfið notar *VM2* hraðalíkanið, sem nálgar betur jarðlagagerð Suðurlands. Með því að bera saman reiknaða ferðatíma frá ákveðnum stað við niðurstöður staðsetningarforrita fyrir sömu ferðatíma, má meta skekkjuvalda m.t.t. mismunandi hraðalíkana og stöðvaneta. Reiknaðir komutímar skjálfta á 5 og 10 km dýpi undir norðaustanverðum Eyjafjallajökli voru staðsettir í Hypoinverse með *VM1* og *VM2* hraðalíkönunum (6. og 7. mynd). Komutímum úr *VM1* og *VM2* var einnig víxlað til þess að meta áhrif frávika í hraðalíkani á staðsetningarnar. Þegar gerður er samanburður á Hypoinverse staðsetningum tilbúinna jarðskjálfta á 0–15 km dýpi kemur í ljós að Hypoinverse ræður ekki við staðsetningar skjálfta grynnri en 3–4 km með öllum stöðvum og grynnri en 7 km með SIL stöðvunum eingöngu (8. mynd). Þegar reiknuðum ferðatímum er víxlað á milli hraðalíkana (neðri myndir) verða dýptarákvarðanir hypoinverse óreglulegri í efstu 5 km. Niðurstöður sýna að frávik í staðsetningum eru að stærstum hluta háðar þéttleika og nálægð stöðvanetsins. Skekkja vegna frávika í hraðalíkönum er stærðargráðu minni. Mælanetið sem sett var umhverfis Eyjafjallajökul í byrjun mars 2010 bætir staðsetningar jarðskjálfta á svæðinu til muna en nær ekki að ákvarða dýpi jarðskjálfta í efstu 6 km með nægilegri upplausn, til þess hefði þurft að setja mæla ofan á upptakasvæðið í austanverðum jöklinum.

REFERENCES

Bai, L., Z. Wu, T. Zhang and I. Kawasaki 2006. The effect of distribution of stations upon location error: Statistical tests based on the double-difference earthquake location algorithm and the bootstrap method. *Earth Planets Space* 58, e9–e12.

Bjarnason, I. Th., W. Menke, Ó. G. Flóvenz and D. Caress 1993. Tomographic image of the Mid-Atlantic plate boundary in southwestern Iceland. *J. Geophys. Res.* 98, 6607–6622.

Bondár, I., S. C. Myers, E. R. Engdahl and E. A. Bergman 2004. Epicentre accuracy based on seismic network criteria. *Geophys. J. Int.* 156, 483–496.

Brandsdóttir, B. and W. H. Menke 2008. The seismic structure of Iceland. *Jökull* 58, 17–35.

Brandsdóttir, B., M. Parsons, R. S. White, Ó. Guðmundsson, J. Drew and B. S. Thorbjarnardóttir 2010. The May 29th 2008 earthquake aftershock sequence within the South Iceland Seismic Zone: Fault locations and source parameters of aftershocks. *Jökull* 60, 23–46.

Drew, J. 2010. *Coalescence Microseismic Mapping: an Imaging Method for the Detection and Location of Seismic Events.* Ph.D. dissertation, University of Cambridge, U.K.

Einarsson, P. and K. Saemundsson 1987. Earthquake epicenters 1982–1985 and volcanic systems in Iceland (map). In: Sigfússon, Th. (ed.), *Í hlutarins eðli: Festschrift for Thorbjorn Sigurgeirsson.* Menningarsjóður, Reykjavík.

Einarsson, P. and Á. R. Hjartardóttir in prep. Structure and tectonic position of the Eyjafjallajökull volcano, southern Iceland.

Gudmundsson, Ó., B. Brandsdóttir, W. H. Menke and G. E. Sigvaldason 1994. The crustal magma chamber of the Katla volcano in south Iceland revealed by seismic undershooting. *Geophys. J. Int.* 119, 277–296.

Jóhannesson H. and K. Sæmundsson 2009. Geological map of Iceland, 1:600 000. Bedrock Geology. Icelandic Institute of Natural History, Reykjavík.

Klein, F. W. 2002. User's guide to Hypoinverse-2000, a FORTRAN program to solve for earthquake locations and magnitudes. *U.S. Geol. Surv. Open File Rep.* 02-171, 123 pp.

Martens, H. R., R. S. White, J. Key, J. Drew, H. Soosalu and S. S. Jakobsdóttir 2010. Dense seismic network provides new insight into the 2007 Upptyppingar dyke intrusion. *Jökull* 60, 47–66.

Óskarsson, B. V. 2009. *The Skerin ridge on Eyjafjallajökull, south Iceland: Morphology and magma-ice interaction in an ice-confined silicic fissure eruption.* M.Sc. dissertation, University of Iceland, 111 pp.

Pálmason, G. 1971. *Crustal Structure of Iceland from Explosion Seismology.* Societas Scientiarum Islandica, Reykjavík, 187 pp.

Sigmundsson, F., S. Hreinsdóttir, A. Hooper, T. Árnadóttir, R. Pedersen, M. J. Roberts, M. Óskarsson, A. Auriac, J. Decriem, P. Einarsson, H. Geirsson, M. Hensch, B. G. Ófeigsson, E. Sturkell, H. Sveinbjörnsson and K. L. Feigl 2010. Intrusion triggering of the 2010 Eyjafjallajökull explosive eruption. *Nature* 468, 426–430, doi:10.1038/nature09558.

Tarasewicz, J., B. Brandsdóttir, R. S. White, M. Hensch and B. Thorbjarnardóttir 2011. Using microearthquakes to track repeated magma intrusions beneath the Eyjafjallajökull stratovolcano, Iceland. *J. Geophys. Res.* doi:10.1029/2011JB008751, in press.

Vogfjörd, K. S., G. Nolet, W. J. Morgan, R. M. Allen, R. Slunga, B. H. Bergsson, P. Erlendsson, G. Foulger, S. Jakobsdottir, B. Julian, M. Pritchard and S. Ragnarsson 2002. Crustal profiling in Iceland using earthquake source arrays. *Eos Trans. AGU. S61C-1161.*

Wessel, P. and W. H. F. Smith 1998. New, improved version of the Generic Mapping Tools released. *EOS Trans. AGU* 79, 579.